The Cryosphere Discuss., 4, 2557–2585, 2010
www.the-cryosphere-discuss.net/4/2557/2010/
doi:10.5194/tcd-4-2557-2010

The Cryosphere Discussions

Dust from the dark region in the western ablation zone of the Greenland ice sheet

I. G. M. Wientjes[1], R. S. W. Van de Wal[1], G. J. Reichart[2,3], A. Sluijs[4], and J. Oerlemans[1]

[1]Institute for Marine and Atmospheric research Utrecht (IMAU), Utrecht University, Princetonplein 5, 3854 CC, Utrecht, The Netherlands
[2]Department of Earth Sciences, Utrecht University, Budapestlaan 4, 3584 CD Utrecht, The Netherlands
[3]Alfred Wegener Institute for Polar and Marine Research, Am Handelshafen 12, 27570, Bremerhaven, Germany
[4]Biomarine Sciences, Institute of Environmental Biology, Utrecht University, Laboratory of Palaeobotany and Palynology, Budapestlaan 4, 3584 CD Utrecht, The Netherlands

Received: 29 November 2010 – Accepted: 6 December 2010 – Published: 10 December 2010

Correspondence to: I. G. M. Wientjes (i.g.m.wientjes@uu.nl)

Published by Copernicus Publications on behalf of the European Geosciences Union.

Abstract

A dark region of tens of kilometres width is present on the western ablation zone of the Greenland ice sheet. The dark appearance is caused by higher amounts of dust. This dust has either been deposited recently or was brought to the surface by outcropping ice. Because the resulting lower albedos may have a significant effect on melt rates, we analysed surface dust, also called cryoconite, from locations in the dark region as well as locations from the brighter surrounding reference ice with microscopic and geochemical techniques to unravel the composition and origin. We find that (part of) the material indeed crops out from the ice, and that there is little difference between dust from the dark region and from the reference ice. Although, the dust from the dark region seems enriched in trace and minor elements that are mainly present in the current atmosphere because of anthropogenic activity. This enrichment is probably caused by higher precipitation and lower melt rates in the dark region relative to the ice marginal zone. The rare earth elemental ratios of the investigated material are approximately the same for all sites and resemble Earths average crust composition. Therefore, the cryoconite does probably not contain volcanic material. The mineralogical composition of the dust excludes Asian deserts, which are often found as provenance for glacial dust in ice cores, as source regions. Consequently, the outcropping dust likely has a more regional origin. Finally, we find cyanobacteria and algae in the cryoconite. Total Organic Carbon accounts for up to 5 weight percentage of the cryoconite from the dark region, whereas dust samples from the reference ice contain only 1% or less. This organic material is likely formed in situ. Because of their high light absorbency, cyanobacteria and the organic material they produce, contribute significantly to the low albedo of the dark region.

TCD

4, 2557–2585, 2010

1 Introduction

The western ablation zone of the Greenland ice sheet contains a region, which is darker than the surrounding ice (Fig. 1). This dark region is situated some tens of kilometres from the margin and stretches from 65° N to 70° N. The dark appearance implies lower albedos and therefore enhanced melt rates. Unravelling the underlying processes that force the low albedo is critical to determine the existence of this region. More knowledge about the dark region will help to predict how this region will develop in the future, and what its influence will be on the mass balance of Greenland.

Accumulation of melt water at the surface could cause the observed dark region, since water might drain slowly due to the cold ice and the small surface slope (Van de Wal and Oerlemans, 1994; Knap and Oerlemans, 1996; Greuell, 2000). However, Wientjes and Oerlemans (2010) compared the spectral signature of the dark region to that of the surrounding brighter ice, showing a pattern that is typical for ice containing more dust. This dust can have two main sources; recent enhanced deposition of dust or accumulation through outcropping of old dust layers. Because the dark region appears every year during the summer season, fixed at the same position at some distance from the margin, the dust unlikely represents only recent dry or wet deposition. In addition, satellite images reveal a wavy pattern in the dark ice, which is typical for the outcropping of tilted, stratified ice layers (Fig. 2). Therefore, the dust was probably initially deposited higher on the ice sheet, travelled through the ice sheet towards the margin and accumulated in the ablation zone (Wientjes and Oerlemans, 2010). In the ablation zone, a horizontal surface ice profile perpendicular to the margin of the ice sheet represents a time line; the closer to the margin, the older the ice (e.g. Reeh et al., 1987). Dust causing the dark region may thus originate from a period when more dust settled in the accumulation zone of the ice sheet. It might have been deposited during cold periods, due to dryer and windier conditions (e.g. Fuhrer et al., 1999; Ruth et al., 2003). Alternatively, the dust could be volcanic material that was deposited on the ice (e.g. Clausen et al., 1997; Mortensen et al., 2005). Reeh et al. (2002) and Petrenko

TCD
4, 2557–2585, 2010

et al. (2005) found bands of dark ice near Jakobshavn, closer to the margin, containing dust from a colder glacial period. A similar dark region has been found in North-East Greenland, probably caused by dust that was deposited high on the ice sheet during the Pleistocene (Bøggild et al., 1996, 2010).

Dust on the ice is often called cryoconite, as suggested by Nordenskjöld (1875). When this dust accumulates on the ice surface, it absorbs sunlight and melts in the ice forming cryoconite holes. The holes deepen until the melt rate at the bottom of these holes equals the ablation rate at the ice surface (Gribbon, 1979). They are typically a few centimetres in diameter, and several centimetres to decimetres deep, water filled and with the cryoconite lying on the bottom (e.g. Gajda, 1958). Because the cryoconite holes contain nutrients released from the dust minerals, water and sunlight, they form an ideal habitat for microorganisms (Wharton et al., 1985). Cryoconite can significantly lower the albedo of the ice surface in the visible part of the spectrum (Takeuchi et al., 2001; Takeuchi, 2009; Bøggild et al., 2010). The locally formed organic matter of the cryoconite is one of the main factors for this albedo lowering. Takeuchi (2002) found that the amount of dark coloured organic substances, possibly the residue of bacterial decomposition of organic matter, determines the optical characteristics of the cryoconite. In addition, the aggregation of dark particles and organic debris by extracellular polymeric substance affects the light absorbency of the cryoconite (Hodson et al., 2010).

To elucidate the origin and characteristics of the surface dust in the dark region, cryoconite from the dark ice as well as from the brighter ice was collected and analysed. We sampled at various locations along the K-transect, a series of surface mass balance and weather station sites in western Greenland (Van de Wal et al., 2005). The sites are situated on a line perpendicular to the ice sheet margin around 67° N, and cover both the dark region (S6, S7 and S8), and the bright ice closer to the margin (S4, SHR and S5), see Fig. 3. In this study, we analysed the shapes and the mineralogical composition of the collected grains (Sect. 3.1), their elemental composition (Sect. 3.2), and the morphology and amount of microorganisms in the cryoconite (Sect. 3.3).

TCD
4, 2557–2585, 2010

2 Material and methods

2.1 Samples

Cryoconite was collected from six sites along the K-transect (Table 1) on 2 and 3 September 2009. The number of samples was restricted by logistical constraints and surface conditions like snow or frozen holes. Table 1 shows the number of samples collected. At S8 we only managed to take small sized samples, which did not yield enough material for the full suite of analyses. At some locations the cryoconite holes were deeper than expected; at S6 they were even about 50 cm deep. Although the holes were variable in depth among the locations, they had similar depths at individual sites, consistent with previous findings (e.g. Gribbon, 1979). At S4, S5 and S6 large patches or streams of dust were present on the surface (Fig. 4). We collected dust from the holes as well as from these dust patches and streams. In between sampling, tools were rinsed with distilled water to prevent cross contamination among the samples. Analyses revealed no significant differences between dust from surface patches and streams, or dust from cryoconite holes.

2.2 Geochemical analyses and microscopy

The cryoconite was studied with an optical microscope as well as a scanning electron microscope (SEM, XL30FEG, FEI). Together with SEM, Energy-Dispersive X-ray spectroscopy (EDX) was performed, to qualitatively determine the bulk mineralogical composition of the individual observed grains. For these measurements, material was mounted on a stub, dried and coated with carbon. The bulk mineralogical composition of the whole samples was qualitatively analysed by X-Ray Diffraction (XRD), using a powder diffractometer (AXS D8 Advance, Bruker) with Co-Kα radiation. The different minerals were identified based on their spectral characteristics.

Total Organic Carbon (TOC) and Nitrogen (N) concentrations were measured using an Elemental Analyser (NA 1500 NCS, Fisons). The material was decalcified prior to

TCD
4, 2557–2585, 2010

analyses by repeated rinsing with 1 M HCl (4 h, 12 h) followed by washing with demineralized water. Concentrations measured on the decalcified residue were back corrected to their original values using the determined weight loss. Because samples from S7 were too small for this procedure, they were decalcified by acidification with 25% HCl in situ within silver sample cups as described in Nieuwenhuize et al. (1994). Based on duplicate analyses and including in-house standards the relative standard deviations for TOC and N were both better than 2% of the recorded weight percentage of TOC.

Total dust samples were dissolved in an acid mixture of 2.5 ml mix acid ($HClO_4$:HNO_3 = 3:2) and 2.5 ml HF, and subsequently evaporated until gel was formed before being taken up again in 25 ml 4.5% HNO_3 suprapur acid. Major elements were quantified using Inductively Coupled Plasma Atomic Emission Spectroscopy (ICP-AES, Varian), minor and trace elements using Inductively Coupled Plasma Mass Spectroscopy (ICP-MS, X-Series II, Thermo Scientific). The elemental concentrations were calibrated against standard solutions. Duplicates were used to calculate relative standard deviations. The precision for all elements shown in this paper is better than 2.5% relatively, with exception of Antimony, Arsenic and Mercury, which have a precision of 7.8%, 8.7% and 12.7% respectively.

3 Results and discussion

3.1 Grain shape and composition

Visual inspection using a light microscope and SEM analyses reveal that the overall grain shapes at the various sites are similar. Most grains have rather angular shapes and are characterized by sharp edges (Fig. 5a). The fragile, acute angles are typical for volcanic material, but have also been observed in glacial grains (Mahaney, 2002). However, the high amounts of these angular-faceted, sharp-edged grains are found in the dark region as well as in the reference ice, where precipitation rates are low and snow is eroded by wind (Van den Broeke et al., 2008). This excludes a single recent

TCD
4, 2557–2585, 2010

volcanic source. The other possibility for volcanic material to reach the ablation zone is settling in the accumulation zone of the ice sheet during periods of volcanic activity, followed by transport through the ice, and subsequent accumulation through prolonged melting in the ablation zone. This outcropping volcanic material would, hence, be enriched in volcanic grains. Still, also grains transported together with the volcanic dust, but originating from different sources should accumulate here. The overwhelming presence of acute edged grain particles, and the lack of rounded grains suggest that these grains became angular and sharp-edged due to glacial transport itself, independent of their origin. Due to the grain tot grain contact in the ice, the grains may suffer abrasion. Abrasion features on some of the grains (see Fig. 5b) confirm that the grains indeed have been transported through the ice. In theory, the material could also be entrained from the underlying bedrock. This seems unlikely, however, as the higher sites (S7 and S8) are located close to the equilibrium line, and particle trajectories through the ice towards these sites do not get close to the bottom. We therefore conclude that at least part of the dust comes from higher parts of the ice sheet, outcropping in the ablation zone.

The chemical composition of individual grains was assessed by EDX, whereas the bulk dust mineralogy was determined using XRD. Although the relative abundance of the various minerals might differ between the sites, all the samples analysed contained largely the same minerals. The EDX showed grains, each consisting of a single mineralogy, mainly quartz, feldspars and plagioclases. A dominant contribution of these 3 minerals to the bulk dust composition is in line with the results of the XRD analyses. The samples mainly consist of quartz and albite with some anorthite. Within these dominant components minor amounts of phyllosilicate were detected as well.

The cryoconite at S4 seems coarser relative to the other sites. Visual interpretation with SEM revealed that material from this site contains larger grains than observed in the other samples. In addition, the EDX analyses indicate that the dust from S4 consists of quartz particles with some feldspars and plagioclases, whereas at other locations, the relative abundances of plagioclases and feldspars seem higher with respect

TCD
4, 2557–2585, 2010

to the quartz concentration. S4 is located close to the margin, allowing for a possible influx of some wind-blown material from the nearby tundra. Possibly even some material entrained from the bedrock has been added to the other grains at this site. The high relative abundance of feldspars and plagioclases relative to the quartz in the samples could be due to a lesser degree of chemical weathering, or a more felsic nature of the source rock for the dust. For this reason, sources that have undergone significant weathering, such as old deserts, can be excluded as the origin of the cryoconite, because they mainly consist of quartz.

Maggi (1997) investigated changes in mineralogy of atmospheric dust in the GRIP ice core spanning the time interval between the Eemian and the last glacial maximum, and found two distinct assemblages with different characteristics during cold and warm episodes. One consists mainly of quartz, illite, chlorite, micas, and feldspars, related to cold mid-high-latitude source areas; and the other consist mainly of kaolinite and Fe (hydr)oxides, related to warm and humid low-latitude source areas. As our samples does not contain kaolinite and as we did not detect any Fe (hydr)oxides-coated grains using EDX, our samples compare most favourably with the first assemblage of Maggi (1997), excluding low-latitude areas as a source for the cryoconite. Svensson et al. (2000) investigated twelve glacial dust samples from the GRIP ice core, and indicated eastern Asia being the main source for these samples originating from the Younger Dryas, the Bølling, the Last Glacial Maximum and cold and mild glacial periods back to 44 kyr B.P. He found higher kaolinite/chlorite ratios and lower feldspar content in the dust from cold glacial periods relative to warmer periods. This is in contrast with the findings by Maggi (1997). However, as the mineralogical composition of our samples differs from the mineralogical composition of all samples from Svensson et al. (2000), eastern Asia does not qualify as the main source for the dust in the dark region. This is probably due to the fact that our samples originate from a period within the Holocene, when circumstances were less dry and windy than during glacial conditions.

TCD
4, 2557–2585, 2010

Summarizing, part of the dust consists of outcropping material that initially settled higher on the ice sheet during dustier periods, although common source areas for glacial dust, like Asian desserts, can be excluded as provenance for this dust.

3.2 Elemental composition

The samples contain similar concentrations of most elements. However, the samples from S6 and S7 contain less inorganic material, because they were diluted by higher amounts of organic matter, as we will explain in Sect. 3.3. To overcome misinterpretation, we corrected for the amount of organic matter in the samples. We have measured the TOC and N concentrations of the samples and we assume that the total organic matter can be described by the mass of CH_2O and N. We multiplied the relative TOC concentrations for each site by 2.5, based on the relative molecular weights ratio of C:CH_2O is 12:30, and add the relative concentration of N. The percentage of organic matter obtained in this way, was used to correct all the results shown in this paper.

When plotting elements against each other, samples seem to cluster into two groups with S4 and S5 in one cluster, and S6 and S7 in the other cluster. This suggests compositional differences between samples from the dark region and from the reference ice, as S6 and S7 are both located in the dark region, whereas S4 and S5 are located in the brighter ice close to the margin. Figure 6 shows this clustering when Tin (Sn) is plotted against Aluminium (Al). The subdivision in two groups is also observed for other elements. The results for SHR are different from both the two clusters, but as there is only one single sample from this site, it is hard to assign a third cluster and draw firm conclusions.

For each element we divided the average concentration for samples from the dark region by the average concentration for samples from the reference ice. Figure 7 shows the results for part of the elements measured with either ICP-AES or ICP-MS. Values above 1 indicate that these elements are relatively enriched in the dark region with respect to the reference ice. Especially Caesium (Cs) is much more abundant in the dark region, but also heavy metals such as Lead (Pb), Antimony (Sb) and Mercury

TCD
4, 2557–2585, 2010

(Hg) have larger concentrations in the dark region. As these are all elements that are relatively enriched in the atmosphere by anthropogenic pollution, a recent source (after industrial revolution) for these elements seems likely. S6 and S7 (the sites in the dark region) are located some tens of kilometres away from the equilibrium line. It is unlikely that dust has travelled this distance through the ice sheet within a short period of about 100 years. Therefore these elements do apparently not originate from the part of the dust that crops out from the ice. This implies recent deposition, which does not show up near S4 and S5, probably because most snow is blown away immediately at these sites, and melt rates are higher with respect to the dark region. In addition, these elements might accumulate due to the uptake by microorganisms, which are much more abundant in the dark region (Sect. 3.3).

Figure 8 shows the rare earth elements (REE) normalized to the averaged upper continental crust (Taylor and McLennan, 1995). The results for each location are averaged. For most of the elements, this value lies close to 1. That means that the average composition of the collected surface dust resembles the average composition of the upper earth crust, as well as the average composition of volcanic material, as most of the upper earth crust originates from volcanic material. However, Icelandic volcanoes show a different pattern and can therefore be excluded as possible origin of this dust. For comparison, the REE pattern from tephra of the February 2000 eruption of Hekla (Moune et al., 2006) is added in Fig. 8. In addition, the REE patterns for the different sampling sites resemble each other closely. REE patterns of dust samples show often more variation, for example glacial dust from ice cores in Antarctica (Basile et al., 1997). As all sites are located at different distance from the margin, the outcropping material originates from different periods. If dust from a single event, like a large volcanic eruption, would have settled in the accumulation zone of the Greenland ice sheet and is outcropping now at one of these sites, it should alter the REE pattern for that specific site. As this is not the case, we exclude a single volcanic eruption as possible provenance for the dust. As the REE patterns for the different sites do not show large variations, they seem to have a common source area, that provide dust to the

TCD
4, 2557–2585, 2010

Greenland ice sheet at all these different periods. This makes a regional source most plausible.

We conclude that the dust from different sites has mainly the same provenance; although dust from the dark region is enriched with elements from the current atmosphere by higher accumulation rates. The outcropping dust seems to have a regional origin.

3.3 Microorganisms

Visual inspection with a light microscope using normal light revealed that the cryoconite also contains microorganisms (Fig. 9). No organisms are present at Site S4 and only small granules containing organic matter were detected in samples from S5. However, samples from all other sites contain long yellow-brownish filamentous strings that represent cyanobacteria (Takeuchi, personal communication). These bacteria are present, not only as loose strings in the samples (Fig. 9a), but are also aggregated in granules, together with mineral particles and organic matter. At S6 these cryoconite granules appeared very dark-coloured using the transmitted light microscope and are therefore large and thick-walled (Fig. 9b), whereas the cryoconite granules from SHR, S7 and S8 were covered with yellow or brown strings of cyanobacteria (Fig. 9c). In addition, we noted abundant occurrence of green algae at the higher altitude sites (Fig. 9d).

The TOC measurements on dry cryoconite confirmed our microscope observations that organic matter was abundantly present at sites from the dark region. Figure 10 shows the averaged percentage of total organic carbon (TOC) and nitrogen (N) for the different sites. The ratio C/N ranges between 11.3 and 13.5 for all the samples from SHR, S6 and S7. Because the TOC and N values are low for the samples from S4 and S5, their C/N ratio is determined by the slope of the trend line through the plotted values of C against N. This is done to overcome misinterpretation as result of small nitrogen leakage during the measurements. The C/N ratio is around 12.2 for the samples from these sites. Takeuchi (2002) found C/N ratios between 9 and 14 (mostly around 11) for different cryoconites of nine glaciers from the Himalaya, Tibet, and the

TCD
4, 2557–2585, 2010

Arctic. In addition, Hodson et al. (2010) found a C/N ratio of 13 ± 1 for cryoconite from Longyearbreen, a valley glacier in Svalbard. Therefore, our findings seem to compare well with these literature values.

Concentrations of TOC and N seem to increase with elevation. All the samples from S4 have a TOC content <0.2 weight percent (%) and all the samples from S5 have a TOC content <0.8% (the lowest value is 0.36%). In contrast, the samples from S6 and S7 contain between 4.5% and 5.5% TOC. From SHR we have only one measurement, indicating a TOC content of 2.6%. The total organic carbon in the dark region (S6 and S7) is rather high. Takeuchi (2002) found values of 0.54–4.37% TOC for the cryoconites from nine different glaciers, with 4.37% for Austre Brøggerbreen in Spitsbergen, Norway and respectively 2.22% and 2.06% for Penny Ice Cap, Greenschield Glacier in Baffin Island and Devon Ice Cap, Sverdrup Glacier in Devon Island, both in Nunavut, Canada. Bøggild et al. (2010) found cryoconite from northeast Greenland containing 5% organic matter, and Takeuchi (2009) found 2.9% to 8.8% organic matter in the surface dust from ice from the Gulkana Glacier, Alaska Range, USA. If we assume that organic matter can be described by the mass of CH_2O, the amount of organic matter corresponding with 5% TOC is 12.5%, calculated by using relative molecular weights. Together with the measured N, this becomes 13%. This value is considerably higher than the values found by Bøggild et al. (2010) and Takeuchi (2009). However, as organic matter might not only contain CH_2O and N, this might be an underestimation, with real values of organic matter being even higher.

It is not obvious why the biological activity increases with altitude. The amounts of useful elements provided by the cryoconite are equal in the dark region with respect to the reference ice. Phosphorus, which is an essential nutrient for the cyanobacteria, is even higher at S4 compared to the other sites. Also the pH of the ice, that might affect the biological activity, is found to be the same at all sites, between 4.6 and 5.2, both in the cryoconite holes as well as in the surrounding supraglacial streams. These values are slightly lower than values for surface ice from the Gulkana Glacier in Alaska, which are between 4.9 and 5.7 (Takeuchi, 2001). At the higher elevations, the ice is

TCD
4, 2557–2585, 2010

also longer covered by snow, which is more likely to reduce algal growing. However, global radiation strongly increases with altitude at the Greenland ice sheet, because of a decreasing cloudiness and a more transparent atmosphere (Konzelmann et al., 1994). This effect might be an important factor for the biological activity.

Stibal et al. (2006) suggest that microorganisms prefer fine sediment in the cryoconite. As the cryoconite at S4 contains coarser material relative to the other sites, this might also contribute to the absence of organisms at S4. Takeuchi (2001) found that the abundance of algae increase with altitude at Gulkana Glacier, Alaska, caused by the outwash of the algae at lower sites where more melt occurred, as the microorganisms on this glacier mainly consist of unicellular green algae that do not form cryoconite granules. However, if aggregations formed with cyanobacteria, organic matter and mineral particles, these granules are more resistant against flushing by melt water Takeuchi (2001). In our case these aggregations formed, and it is very unlikely that they completely washed out at S4, were we found no microorganisms but considerable amounts of dust. We also found green algae, which were only abundant at the higher elevations. In contrast to the cyanobacteria, these green algae could be flushed away from the glacier at the lower sites, due to the higher melt rates.

Despite the fact that it is uncertain what causes the occurrence of cryoconite granules at higher altitudes, it is well known that they have a high light absorbency (e.g. Takeuchi et al., 2001). As there are abundant of these granules in the dark region, we can conclude that biological activity will certainly contribute to the surface darkening process.

4 Conclusions and discussion

In order to find out more about the characteristics of cryoconite from the dark region, surface material was collected and analyzed from locations inside the dark region, and from locations of brighter ice closer to the ice margin. Using transmitted light microscopy as well as electron microscopy, we observed triangular-faceted, sharp-edged

TCD
4, 2557–2585, 2010

grains, which are either volcanic or glacial grains, both indicating glacial transport. This implies that at least part of the dust is outcropping from the ice, in the dark region as well as in the reference area. Geochemical analyses revealed that the mineralogical and elemental composition of the material is mostly the same for both areas. However, enrichment with elements from anthropogenic sources in the dark region suggests an influence from recent atmospheric material by precipitation.

In addition, abundant green algae and cyanobacteria, forming cryoconite granules, were found in the dark region. The relative amount of microorganisms in this region is much higher compared to the reference ice. It is not quite clear what causes these differences, although global radiation, sediment texture and meltwater supply might play a role. The TOC values found for the dark region are high compared to literature values. As the organic matter in the cryoconite is well known to have a high light absorbency, the dark region is not only caused by outcropping dust, but biological activity also significantly contributes to the darkening of the surface.

The REE patterns for the different sites reveal a source with a chemical composition similar to the upper continental crust. Therefore, the material does not seem to contain meteorites, which are found incidentally on the Greenland ice sheet in relatively high amounts (Maurette et al., 1987). Besides, meteorites were not revealed by the microscopy at all, and seem therefore not present in the dust samples. The outcropping dust could be volcanic material, but as the dark region is several tens of km wide, a series of several eruptions are more likely to have caused the dark region than one single big eruption. However, nearby Icelandic volcanoes provide a different REE pattern and are therefore excluded as possible source. Comparison of the mineralogical composition of the dust with literature values shows that the samples do not contain material from Asian deserts, which is often found in ice cores during glacial periods. For these reasons, it is most likely that this dust has a regional origin. Coarser grains found at S4 suggest that some recent local wind-blown or bed-rock entrained material is added at this site. However, as the material from the samples from this site shows the same geochemical composition as the other samples, this confirms the idea that all

TCD
4, 2557–2585, 2010

the investigated dust has a local source. Therefore, the dark region is probably caused by higher amounts of local dust, during periods when more dust settles in the accumulation zone of the ice sheet. Together with this dust, microorganisms could have settled on the ice sheet, outcropping at present in the dark region and multiplying rapidly.

To find out more about the origin of outcropping dust, ice cores from several meters need to be analysed, at some depth below the surface to avoid influence from recent dry or wet deposition. Such cores will also provide quantitative information about the amounts of outcropping dust. Also grain size sorting might reveal information about the origin of the dust. For example, Bøggild et al. (2010) found clay size grains in cryoconite from northeast Greenland, revealing dust from Pleistocene origin. Analyses revealing the age of the outcropping dust could provide information about the period in which the dust has settled on the ice sheet. More investigation about the development of microorganisms in the ice could be useful as well. It is likely that higher amounts of dust in the dark region positively influence the absolute amounts of organic matter. Because of their high light absorbency, cyanobacteria and the organic material they produce contribute to the dark colour of the region providing a potential important positive biological feedback on the ice melt by enhancing the albedo lowering of the dark region.

Acknowledgements. We thank C. van der Veen, W. Boot, H. Snellen and P. Smeets for their technical support with the field equipment. We are also grateful to D. van der Meent, H. de Waard, A. van Leeuwen, T. Bouten, A. van Dijk and E. van Vilsteren for their help with the geochemical analysis. J. van Tongeren and L. Bik kindly assisted with the optical microscopy. P. Mason and N. Takeuchi are thanked for useful suggestions. A. Sluijs acknowledges support from the Netherlands Organisation for Scientific Research (NWO-Veni grant 863.07.001) and the European Research Council under the European Community's Seventh Framework Programme (FP7/2007–2013)/ERC Grant agreement no. 259627. Financial support for this work is also provided through the Spinoza-grant and the KNAW-Professorship of J. Oerlemans.

TCD
4, 2557–2585, 2010

References

Basile, I., Grousset, F. E., Revel, M., Petit, J. R., Biscaye, P. E., and Barkov, N. I.: Patagonian origin of glacial dust deposited in East Antarctica (Vostok and Dome C) during glacial stages 2, 4 and 6, Earth Planet. Sci. Lett., 146, 573–589, 1997. 2566

Bøggild, C. E., Oerter, H., and Tukiainen, T.: Increased ablation of Wisconsin ice in eastern north Greenland: observations and modelling, Ann. Glaciol., 23, 144–148, 1996. 2560

Bøggild, C. E., Brandt, R. E., Brown, K. J., and Warren, S. G.: The ablation zone in northeast Greenland: ice types, albedos and impurities, J. Glaciol., 56, 101–113, 2010. 2560, 2568, 2571

Clausen, H. B., Hammer, C. U., Hvidberg, C. S., Dahl-Jensen, D., Steffensen, J. P., Kipfstuhl, J., and Legrand, M.: A comparison of the volcanic records over the past 4000 years from the Greenland Ice Core Project and Dye 3 Greenland ice cores, J. Geophys. Res., 102, 26707–26723, 1997. 2559

Fuhrer, K., Wolff, E. W., and Johnsen, S. J.: Timescales for dust variability in the Greenland Ice Core Project (GRIP) ice core in the last 100,000 years, J. Geophys. Res., 104, 31043–31052, 1999. 2559

Gajda, R. T.: Cryoconite phenomena on the Greenland ice cap in the Thule area, Can. Geogr., 3, 35–44, 1958. 2560

Greuell, W.: Melt-water accumulation on the surface of the Greenland ice sheet: effect on albedo and mass balance, Geogr. Ann. A, 82, 489–498, 2000. 2559

Gribbon, P. W. F.: Cryoconite holes on Sermikavsak, West Greenland, J. Glaciol., 22, 177–181, 1979. 2560, 2561

Hodson, A., Cameron, K., Bøggild, C., Irvinne-Fynn, T., Langford, H., Pearce, D., and Banwart, S.: The structure, biological activity and biogeochemistry of cryoconite aggregates upon an Arctic valley glacier: Longyearbreen, Svalbard, J. Glaciol., 56, 349–361, 2010. 2560, 2568

Knap, W. H. and Oerlemans, J.: The surface albedo of the Greenland ice sheet: satellite-derived and in situ measurements in the Søndre Strømfjord area during the 1991 melt season, J. Glaciol., 42, 364–374, 1996. 2559

Konzelmann, T., van de Wal, R. S. W., Greuell, W., Bintanja, R., Henneken, E. A. C., and Abe-Ouchi, A.: Parameterization of global and longwave incoming radiation for the Greenland Ice Sheet, Global Planet. Change, 9, 143–164, 1994. 2569

Maggi, V.: Mineralogy of atmospheric microparticles deposited along the Greenland Ice Core

TCD
4, 2557–2585, 2010

Project ice core, J. Geophys. Res., 102, 26725–26734, 1997. 2564
Mahaney, W. C.: Atlas of sand grain surfae textures and applications, Oxford University Press, Oxford, United Kingdom, 2002. 2562
Maurette, M., Jéhanno, C., Robin, E., and Hammer, C.: Characteristics and mass distribution of extraterrestrial dust from the Greenland ice cap, Nature, 328, 699–702, 1987. 2570
Mortensen, A. K., Bigler, M., Grönvold, K., Steffensen, J. P., and Johnsen, S. J.: Volcanic ash layers from the Last Glacial Termination in the NGRIP ice core, J. Quaternary Sci., 20, 209–219, 2005. 2559
Moune, S., Gauthier, P. J., Gislason, S. R., and Sigmarsson, O.: Trace element degassing and enrichment in the eruptive plume of the 2000 eruption of Hekla volcano, Iceland, Geochim. Cosmochim. Ac., 70, 461–479, 2006. 2566
Nieuwenhuize, J., Maas, Y. E. M., and Middelburg, J. J.: Rapid analysis of organic carbon and nitrogen in particulate materials, Mar. Chem., 45, 217–224, 1994. 2562
Nordenskjöld, N. E.: Cryoconite found 1870, July 19th-25th, on the inland ice, east of Auleitsivik Fjord, Disco Bay, Greenland, Geol. Mag., Decade 2, 157–162, 1875. 2560
Petrenko, V. V., Severinghaus, J. P., Brook, E. J., Reeh, N., and Schaefer, H.: Gas records from the West Greenland ice margin covering the Last Glacial Termination: a horizontal ice core, Quat. Sci. Rev., 25, 865–875, 2005. 2559
Reeh, N., Thomsen, H. H., and Clausen, H. B.: The Greenland ice-sheet margin – a mine of ice for paleo-environmental studies, Palaeogeogr., Palaeoclimatol., Palaeocol., 58, 229–234, 1987. 2559
Reeh, N., Oerter, H., and Thomsen, H. H.: Comparison between Greenland ice-margin and ice-core oxygen-18 records, Ann. Glaciol., 35, 136–144, 2002. 2559
Ruth, U., Wagenbach, D., Steffensen, J. P., and Bigler, M.: Continuous record of microparticle concentration and size distribution in the central Greenland NGRIP ice core during the last glacial period, J. Geophys. Res., 108, 4098, doi:10.1029/2002JD002376, 2003. 2559
Stibal, M., Šabacká, M., and Kaštovská, K.: Microbial Communities on Glacier Surfaces in Svalbard: Impact of physical and chemical properties on abundance and structure of cyanobacteria and algae, Microb. Ecol., 52, 644–654, 2006. 2569
Svensson, A., Biscaye, P. E., and Grousset, F. E.: Characterization of late glacial continental dust in the Greenland Ice Core Project ice core, J. Geophys. Res., 105, 4637–4656, 2000. 2564
Takeuchi, N.: The altitudinal distribution of snow algae on an Alaska glacier (Gulkana Glacier

TCD
4, 2557–2585, 2010

in the Alaska Range), Hydrol. Process., 15, 3447–3459, 2001. 2568, 2569
Takeuchi, N.: Optical characteristics of cryoconite (surface dust) on glaciers: the relationship between light absorbency and the property of organic matter contained in the cryoconite, Ann. Glaciol., 34, 409–414, 2002. 2560, 2567, 2568
Takeuchi, N.: Temporal and spatial variations in spectral reflectance and characteristics of surface dust on Gulkana Glacier, Alaska Range, J. Glaciol., 55, 701–709, 2009. 2560, 2568
Takeuchi, N., Kohshima, S., and Seko, K.: Structure, formation, and darkening process of albedo reducing material (cryoconite) on a Himalayan glacier: a granular algal mat growing on the glacier, Arct. Antarct. Alp. Res., 33, 115–122, 2001. 2560, 2569
Taylor, S. R. and McLennan, S. M.: The geochemical evolution of the continental crust, Rev. Geophys., 33, 241–265, 1995. 2566
Van de Wal, R. S. W. and Oerlemans, J.: An energy balance model for the Greenland ice sheet, Global Planet. Change, 9, 115–131, 1994. 2559
Van de Wal, R. S. W., Greuell, W., Van den Broeke, M. R., Reijmer, C. H., and Oerlemans, J.: Surface mass-balance observations and automatic weather station data along a transect near Kangerlussuaq, West Greenland, Ann. Glaciol., 42, 311–316, 2005. 2560
Van de Wal, R. S. W., Boot, W., Van de Broeke, M. R., Smeets, P., Reijmer, C. H., Donker, J. J. A., and Oerlemans, J.: Large and rapid melt-induced velocity changes in the ablation zone of the Greenland ice sheet, Science, 321, 5885, 111–113, 2008. 2578
Van den Broeke, M., Smeets, P., Ettema, J., van der Veen, C., van de Wal, R., and Oerlemans, J.: Partitioning of melt energy and meltwater fluxes in the ablation zone of the west Greenland ice sheet, The Cryosphere, 2, 179–189, doi:10.5194/tc-2-179-2008, 2008. 2562
Wharton, R. A., McKay, C. P., Simmons, G. M., and Parker, B. C.: Cryoconite holes on glaciers, BioScience, 35, 499–503, 1985. 2560
Wientjes, I. G. M. and Oerlemans, J.: An explanation for the dark region in the western melt zone of the Greenland ice sheet, The Cryosphere, 4, 261–268, doi:10.5194/tc-4-261-2010, 2010. 2559, 2577

TCD
4, 2557–2585, 2010

Table 1. Characteristics of sample locations.

	Site 4	Site 5	SHR	Site 6	Site 7	Site 8
Height (m a.s.l.)	390	490	710	1020	1110	1260
Distance from margin (km)	3	6	14	37	52	63
Number of samples	6	7	1	6	4	–

TCD
4, 2557–2585, 2010

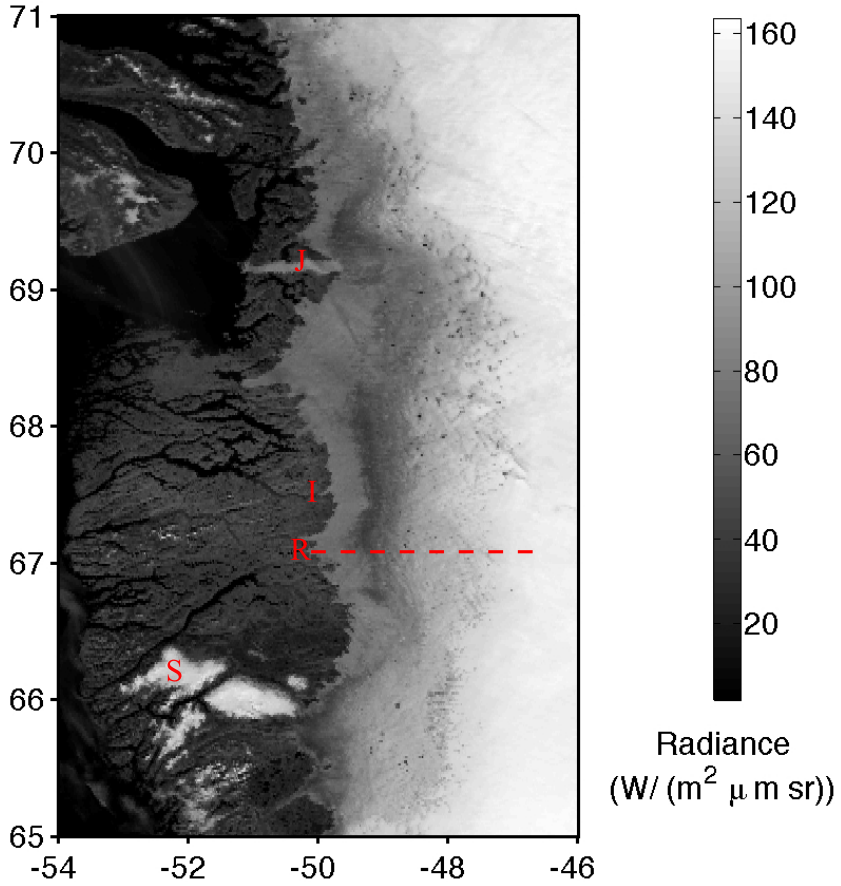

Fig. 1. MODIS image form 9 August 2007, band 2 (841–876 nm), showing the dark region in the ablation zone of west Greenland. S is Sukkertoppen Iskappe, J is Jakobshavn Isbrae, I is Inugpait Qûat, and R is Russell glacier, the starting point of the K-transect (dashed line). Latitudes and longitudes are shown along the axes.

TCD
4, 2557–2585, 2010

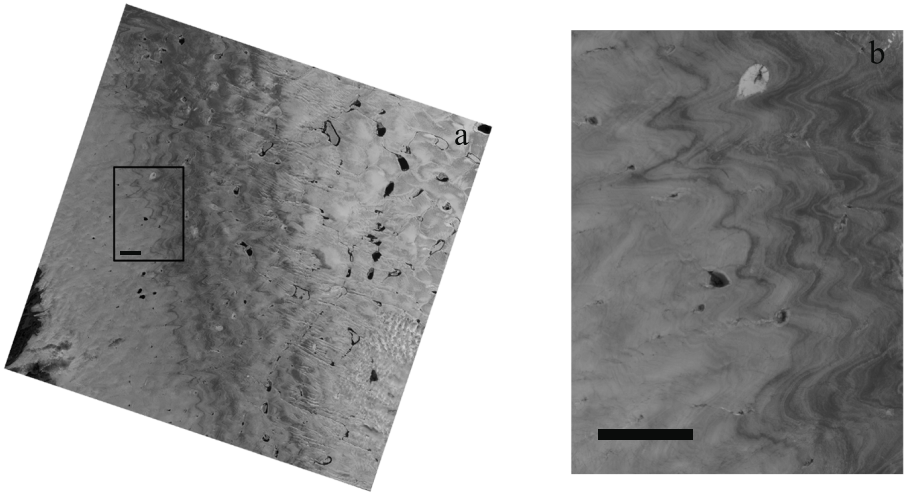

Fig. 2. **(a)** Aster image from 21 July 2002, adapted from Wientjes and Oerlemans (2010) (©METI and NASA [2002]). The glacier in the left corner is Inugpait Qûat (see Fig. 1). **(b)** Inset of panel **(a)**. The scale bar is approximately 3 km. Panel **(b)** clearly shows a wavy pattern indicating outcropping stratified ice layers.

TCD
4, 2557–2585, 2010

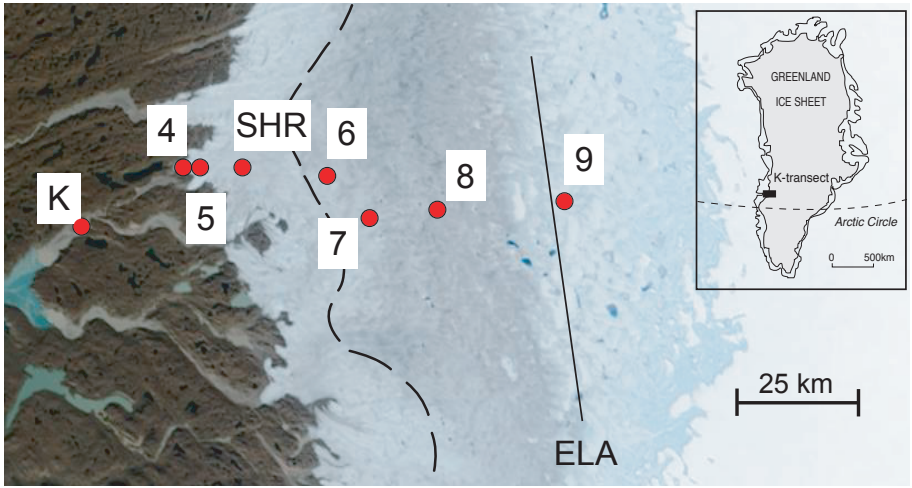

Fig. 3. The K-transect in west Greenland at 67° N, adapted from Van de Wal et al. (2008). The background is a true color composition of NASAModis/Terra from 26 August 2003. K is Kangerlussuaq and 4, 5, SHR, 6, 7, 8 and 9 are surface mass balance sites. The dashed line indicates the western border of the dark region. ELA is the Equilibrium Line Altitude. Sites 4, 5 and SHR are in the brighter reference ice whereas Site 6, 7 and 8 are located in the dark region.

TCD
4, 2557–2585, 2010

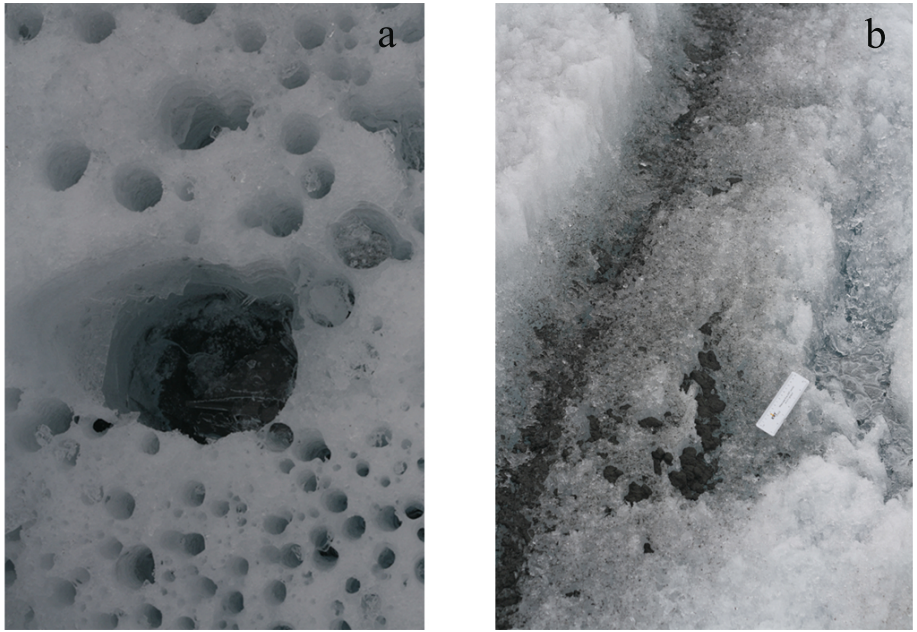

Fig. 4. Photos of the dust in the field. **(a)** Cryoconite holes at S5; the big hole has a diameter of ~12 cm. **(b)** Dust on the ice surface at S5; the white ruler to the right is ~15 cm long. Part of this dust seems to form a stream along a small hummock.

TCD
4, 2557–2585, 2010

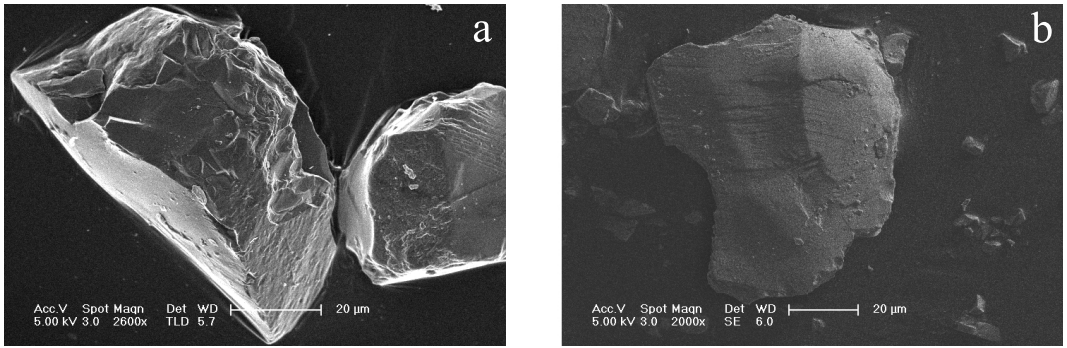

Fig. 5. (a) Sharp-edged and angular grain from S5. **(b)** Grain with abrasion features from S8.

TCD
4, 2557–2585, 2010

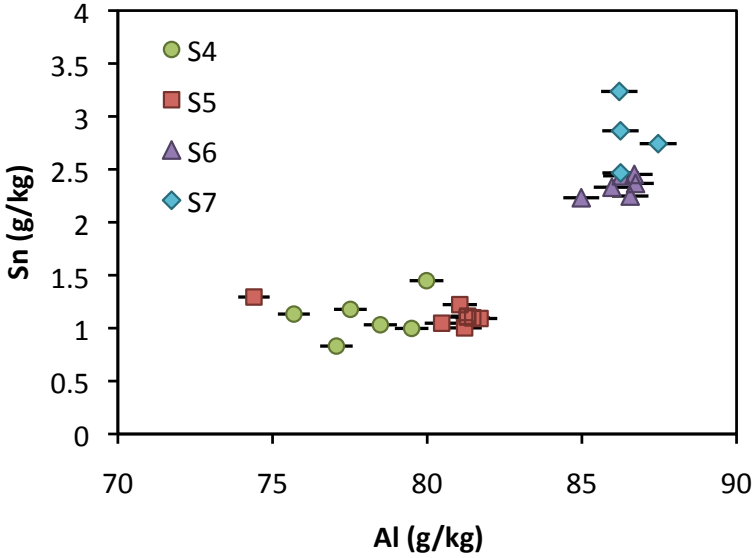

Fig. 6. Tin (Sn) versus Aluminium (Al) for the samples from four different locations.

TCD
4, 2557–2585, 2010

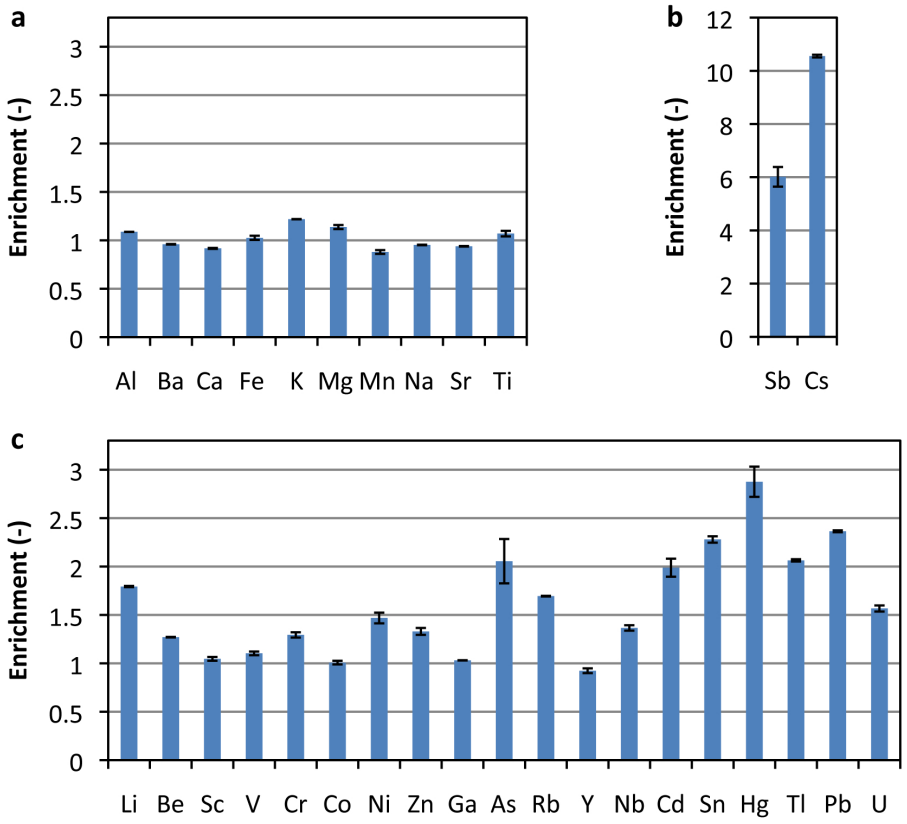

Fig. 7. Enrichment of elements for the dark region, calculated as the average concentration for samples from the dark region by the average concentration for samples from the reference ice. Panel **(a)** shows elements measured with ICP-AES and panel **(b)** and **(c)** shows elements measured with ICP-MS. Error bars represent one standard deviation. Note the different scale in panel **(b)**.

TCD
4, 2557–2585, 2010

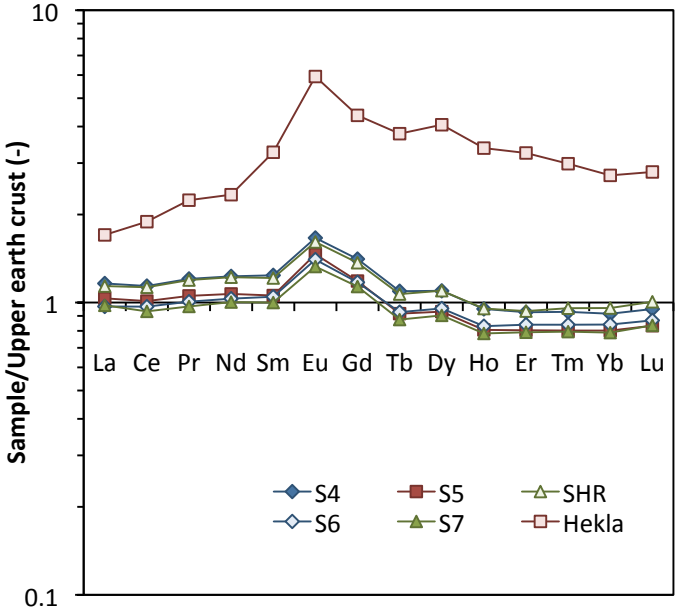

Fig. 8. Rare earth element pattern of the averaged concentration for each location normalized to the upper continental crust. Tephra from the 2000 Hekla eruption is shown for comparison.

TCD
4, 2557–2585, 2010

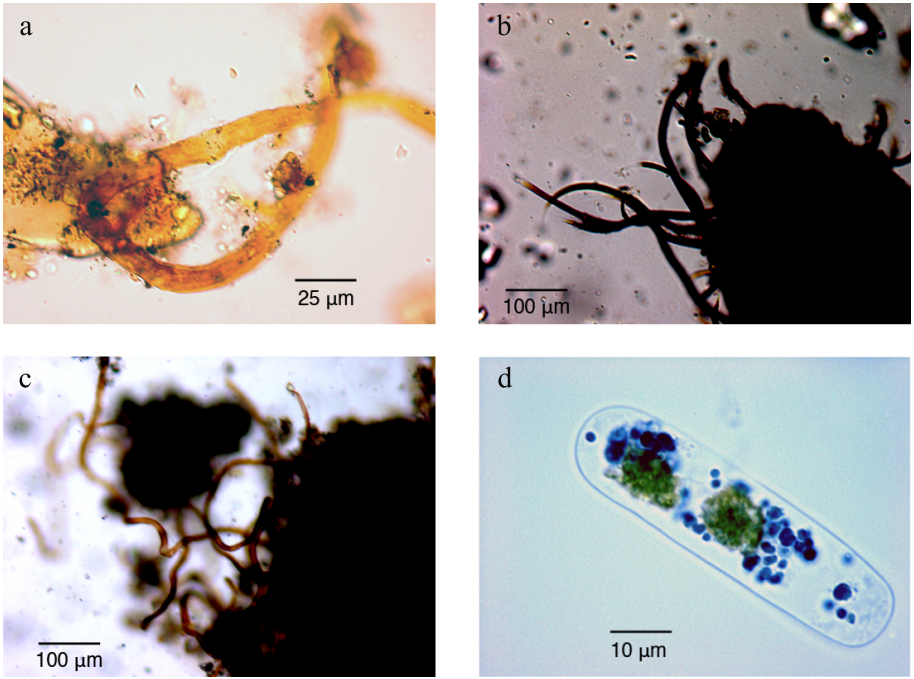

Fig. 9. Microorganisms in the cryoconite. **(a)** Filamentous cyanobacteria. **(b)** Cryoconite granule with black cyanobacteria. **(c)** Cryoconite granule with brown cyanobacteria. **(d)** Green alga.

TCD
4, 2557–2585, 2010

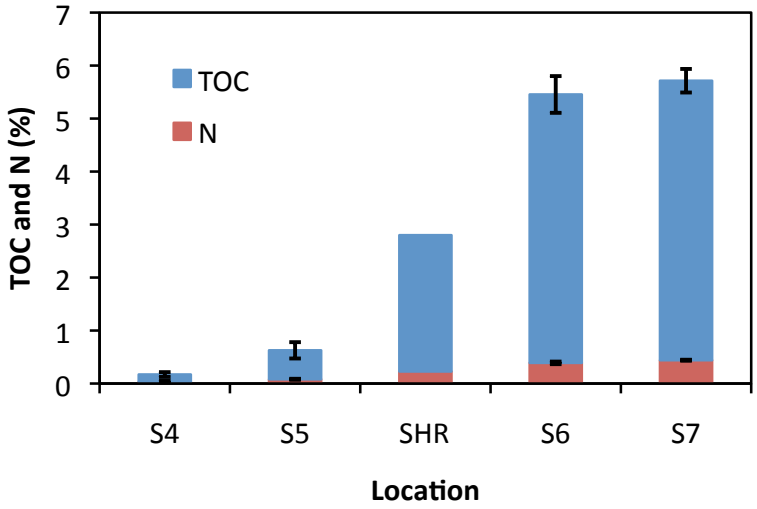

Fig. 10. The averaged concentrations of total organic carbon (TOC) and nitrogen (N) for each location; error bars represent one standard deviation.

TCD
4, 2557–2585, 2010